Published in final edited form as:
Chem Res Toxicol. 2012 February 20; 25(2): 374–380. doi:10.1021/tx2004322.

Induction of ovarian cancer and DNA adducts by dibenzo[*a,l*]pyrene in the mouse

Kun-Ming Chen[1], **Shang-Min Zhang**[1], **Cesar Aliaga**[1], **Yuan-Wan Sun**[1], **Timothy Cooper**[2], **Krishnegowda Gowdahalli**[3], **Junjia Zhu**[4], **Shantu Amin**[3], and **Karam El-Bayoumy**[1]

[1]Dept. of Biochemistry and Molecular Biology, Penn State College of Medicine, Hershey, PA 17033

[2]Dept. of Comparative Medicine, Penn State College of Medicine, Hershey, PA 17033

[3]Dept. of Pharmacology, Penn State College of Medicine, Hershey, PA 17033

[4]Dept. of Public Health Sciences, Penn State College of Medicine, Hershey, PA 17033

Abstract

Tobacco smoking is an etiological factor of ovarian cacner; however, the mechanisms remain largely undefined. Therefore, as an initial investigation we examined the carcinogenicity and DNA adducts formation in the ovary of mice treated with DB[*a,l*]P, a tobacco smoke constituent and environmental pollutant. Ovarian tumors in B6C3F1 mice were induced by direct application of DB[*a,l*]P (24, 12, 6, and 3 nmol/mouse, 3 times a week for 38 weeks) into the oral cavity of mice. At 6 nmol, DB[*a,l*]P induced the highest total ovarian tumor incidence (79%), but the incidence of malignancy was only 15%. However, at the dose of 12 nmol, the total ovarian tumor incidence was 75%, and the incidence of malignancy was 65%. In addition to ovarian tumors, at the dose of 24 nmol, DB[*a,l*]P induced lesions in sites distal from the ovaries including the skin, mammary, lung, and oral tissues which were rare at doses lower than 24 nmol. Another bioassay was conducted to detect and quantify DNA-adducts induced by DB[*a,l*]P (24 nmol, 3 times a week for 5 weeks) in the ovary at 48 h, 1, 2 and 4 weeks after the last administration of DB[*a,l*]P. DNA was isolated, and the dibenzo[*a,l*]pyrene-11,12-dihydrodiol-13,14-epoxide (DB[*a,l*]PDE)-DNA adducts were analyzed by a LC-MS/MS method. DB[*a,l*]P resulted in the formation of (−)-*anti-cis*-DB[*a,l*]PDE-dA and (−)-*anti-trans*-DB[*a,l*]PDE-dA adducts, which were 0.8 and 1.6 fmol/10^6 dA respectively in ovaries of mice within 48 h, and the level of adducts decreased over a week. Our results indicated that DB[*a,l*]P can be metabolized to form (−)-anti-DB[*a,l*]PDE; the latter may, in part, account for DB[*a,l*]P-induced ovarian cancer. This animal model should assist to better understand the mechanisms, account for the induction of ovarian cancer by tobacco carcinogens, and facilitate the development of chemopreventive agents against ovarian cancer.

Keywords

DB[*a,l*]P; ovarian cancer; tobacco smoking

Introduction

Ovarian cancer causes more deaths than any other cancer of the female reproductive system; 15,460 deaths are expected in the US in 2011,[1] and ovarian cancer is the fifth leading cause

Corresponding authors, Kun-Ming Chen (kzc3@psu.edu) and Karam El-Bayoumy (kee2@psu.edu), Dept. of Biochemistry and Molecular Biology, Penn State University College of Medicine, Hershey, PA, 17033.

of cancer deaths among women[2,3]. There are usually no obvious symptoms of early ovarian cancer; therefore, only 15% of ovarian cancers are diagnosed in the localized stage. Although the death rates for ovarian cancer have been decreasing by 1.4% per year since 2002, the five-year survival rate for ovarian cancer patients is 46%.[1,2]

The etiology of ovarian cancer is multifactorial and remains largely undefined; furthermore, the mechanisms by which this disease progresses to more malignant phenotype are poorly understood.[4] The most important risk factor is family history of breast or ovarian cancer.[1,5] Women had breast cancer or have tested positive for inherited mutations in BRCA1 or BRCA2 genes are also at increased risk.[1,6] Other risk factors include hereditary nonpolyposis colon cancer, use of hormones, obesity, nutrition and lifestyles.[1,7] Recent epidemiologic studies also showed sufficient evidence that tobacco smoking causes cancer of the ovary.[1,6,8–10] Epithelial ovarian cancer are divided into several histological subtypes, including serous, mucinous, endometrioid, clear cell, and other less common forms.[11] Among them, advanced-stage mucinous ovarian cancer patients had a worse prognosis than women with non-mucinous epithelial ovarian cancers.[12,13] There is a positive relationship between mucinous tumors and tobacco smoking;[8,9,14–16] based on a large population-based study, this association is increased for current smokers and with increasing number of pack-years.[8] An association between mucinous ovarian cancer with ex-smoker has also been reported.[16] Interestingly, consumption of alcohol is also considered a risk factor for mucinous but not nonmucinous epithelial ovarian cancer.[7,17] Therefore, animal models using agents relevant to etiological factors of the disease would provide valuable tools to better understand the mechanisms that can account for the induction of ovarian cancer and develop suitable approaches for cancer prevention.

The induction of ovarian cancer in laboratory animals by the synthetic carcinogen, 7,12-dimethyl-benz[*a*]anthracene (DMBA), in rodents has served as in vivo models to examine the etiology of the disease and to identify agents that can suppress ovarian carcinogenesis.[18–20] Literature data suggests that diol-epoxide metabolites of polycyclic aromatic hydrocarbon (PAH), such as dibenzo[*a,l*]pyrene DB[*a,l*]P) and benzo[a]pyrene (B[*a*]P), can covalently bind to DNA of ovarian cells from human exposed to cigarette smoke.[21] Although the levels of DB[*a,l*]P are lower than B[*a*]P in samples derived from environmental sources,[22] the fjord region DB[*a,l*]P is the most potent carcinogenic PAH found in tobacco smoke to date in rodent model systems.[23] DB[*a,l*]P is generated from incomplete combustion and has been identified in mainstream cigarette smoke, soil and diesel exhaust particulate matter.[24–26] Consistent with its carcinogenicity, DB[*a,l*]P was also found to induce 6- and 9-fold greater DNA adduct levels than B[*a*]P or DMBA in rat mammary glands at equimolar dose.[27] In addition, Buters et al. found DB[*a,l*]P administered intragastrically induced ovarian tumors in over 70% of the mice, which is the highest among all targeted organs;[28] however, the design of this study was limited to a single dose.

In the current dose-response study, we further confirmed that the ovary is the main target organ of DB[*a,l*]P in the mouse. This model will allow the development of better methods for the early detection and novel chemopreventive agents. We also demonstrated that the tobacco smoke component, DB[*a,l*]P, is involved in the carcinogenesis of ovarian cancer, at least in part, through the formation of DB[*a,l*]PDE-DNA adducts, which were detected for the first time in the ovaries of mice treated with DB[*a,l*]P using a stable isotope dilution LC-MS/MS method that was recently developed in our laboratory.[29]

Materials and Methods

Caution

DB[*a,l*]P and DB[*a,l*]PDE are mutagenic and carcinogenic. They should be handled with extreme care, following safety guidelines.

Chemicals

DB[*a,l*]P and (±)-*anti*-DB[*a,l*]PDE were prepared according to a published method by our group.[30] These chemicals were characterized on the basis of NMR and high-resolution mass spectral data and their purity (≥99%) was determined by HPLC.

(±)-*anti*-DB[*a,l*]PDE-N^6-dA adducts as well as its ^{15}N-labeled counterpart were prepared according to our previously published method.[29] In brief, they were synthesized by reacting 10 μmol of ±)-*anti*-DB[*a,l*]PDE in dry DMF (400 μL) under N_2 with 152 μmol of unlabeled or ^{15}N-labeled dA Spectra Stable Isotopes, Columbia, MD), at 100 °C for 30 min. The resulting mixture was then dried in vacuo, and then dissolved in DMSO/CH_3OH (1:1). The adducts were purified on a reversed-phase YMC ODS-AQ 5 μm, 120 Å column (6.0 mm × 250 mm) (YMC, Wilmington, NC), using a CH_3CN/H_2O gradient on an Agilent series 1100 HPLC system (Agilent Technologies, Palo Alto, CA).[29] The resulting fractions were further purified isocratically with 70% CH_3OH/H_2O. The structure and stereochemistry of adducts were confirmed by a combination of UV, MS, ^1H NMR and CD spectra analysis. The concentration of each purified stereoisomer was determined by UV spectroscopy, ε=43000 cm^{-1} Beckman Coulter DU 640 spectrophotometer).[20] Solvents, other chemicals and enzymes used in the present study were obtained from Sigma-Aldrich (St. Louis, MO).

Animals

Female $B6C3F_1$ (Jackson Laboratories, Bar Harbor, ME) 6 weeks of age, were used in carcinogenesis study. Mice were quarantined for 1 week; then they were transferred to the bioassay laboratory. All mice were kept on a 12-h light:12-h dark cycle, maintained at 50% relative humidity and 21 ± 2°C, and were fed a semi-purified, modified AIN-93M diet (5% corn oil), and water *ad libitum*. The bioassay was carried out in accordance with the NIH Guide for the Care and Use of Laboratory Animals and was approved by Institutional Animal Care and Use Committee.

Animal Treatment

In the carcinogenesis bioassay, female B6C3F1 mice (20/group) at the age of 8 weeks old received DB[*a,l*]P in DMSO, or DMSO alone administered into the oral cavity 3 times a week for 38 weeks or left untreated. The doses used were 24, 12, 6, 3 and 0 nmol/mice each application, and they are equal to 0.29, 0.15, 0.073, 0.035 and 0 mg/kg body weight. Mice were weighed weekly until termination at 47 weeks after the first carcinogen administration. During the progress of the bioassay, mice were culled from the group and sacrificed if we observed a sudden weight loss of more than 20 % or a tumor size exceeding 2 cm in diameter. At termination, mice were sacrificed by carbon dioxide asphyxiation and ovaries were collected and fixed in 10% neutral buffered formalin. Tissues were processed in an automated Tissue-Tek VIP processor and paraffin-embedded with a Tissue-Tek TEC embedding station. Sections were cut at 6 μm for routine hematoxylin and eosin (H&E) staining. All tissues were examined by an ACVP diplomate pathologist blinded to treatments.

In the bioassay for the DNA adducts formation and disappearance, we carried out a time-course study, in which mice were administered with 24 nmol DB[*a,l*]P into the oral cavity 3 times per week for 5 weeks. Six animals per group were sacrificed at 48 h, 1, 2 and 4 weeks

after the last administration of DB[*a,l*]P. At termination, mice were sacrificed by CO_2 asphyxiation and ovarian tissues were collected for DNA adduct analysis.

DNA isolation

DNA was isolated from tissues using the Qiagen genomic DNA isolation procedure. Homogenized tissues were incubated with RNase A and proteinase K for 2h. The DNA was purified with Qiagen genomic tips (500/G). DNA was dissolved in TE buffer (pH=8.0). The concentration was determined by the absorbance at 260 nm using a NanoDrop ND-1000 spectrophotometer (NanoDrop Technologies, Wilmington, DE).

DNA hydrolysis and solid phase extraction

Prior to enzymatic digestion, 200 pg of each [$^{15}N_5$]-*anti-trans*- and [$^{15}N_5$]-*anti-cis*-DB[*a,l*]PDE-dA adducts were added to 200 μg DNA. To the resulted solution, 1M $MgCl_2$ (10 μL/mg DNA) and DNase I (0.2 mg/mg DNA) were added and incubated at 37 °C for 1.5 h. Immediately, nuclease P1 (20 μg/mg DNA) was added and the mixture was incubated at 37 °C for another 1.5 h. After adjusting the pH to 9 using 0.1 M tris buffer (pH=9.0), snake venom phosphodiesterase (0.08 unit/mg DNA) and alkaline phosphatase (2 units/mg DNA) were then added. The mixture was incubated at 37 °C overnight (~ 18 h).[21] The DNA hydrolysate was centrifuged at 14000 rpm for 10 min. Aliquot of the supernatant was subjected to dA base analysis by HPLC. The remaining supernatant was partially purified by solid phase extraction using an Oasis HLB column (1 cm^3, 30 mg, Waters Ltd.). The column was initially conditioned with 1.0 ml of methanol followed by 1.0 ml of HPLC grade water. The digested DNA sample was then loaded onto the column and washed with 1.0 ml of methanol: water (5:95 v/v).[22] The fractions containing DB[*a,l*]PDE-dA adducts were eluted from the column with methanol, then concentrated under mild N_2 stream.

LC-MS/MS analysis

The method used for the detection of DB[*a,l*]PDE-dA adducts by LC-MS/MS is identical to our previously published procedure.[29] In brief, the analysis was carried out on an API 3200™ LC/MS/MS triple quadrupole mass spectrometer interfaced with an Agilent 1200 series HPLC using an Agilent extend-c18 5 μm 4.6 × 150 mm column. The electrospray ionization (ESI) was performed in the positive mode. The MS parameters were set as follows: electrospray source temperature and voltage were 400°C and 5.5 kV, respectively; the declustering potential (DP), collision energy (CE), entrance potential (EP), and cell exit potential (CXP) were optimized as 56, 33, 7.5 and 8 ev, respectively; the collision activated dissociation (CAD) gas was set at 5 psi, while the curtain gas was set at 20 psi. The elution solvent program was 200 ul/min gradient using solvent A (methanol containing 0.1% formic acid) and solvent B (water containing 0.1% formic acid). The gradient was 10% A to 70% A in 5 min, followed by 70% A in 10 min, continued to 90% A in 30 min, and 90% A was held for another 5 min. Adducts were monitored in multiple reaction monitoring (MRM) mode. The MS/MS transitions of *m/z* 604→ *m/z* 335, and *m/z* 609→ *m/z* 335 were monitored for targeted adducts and internal standards, respectively.

Statistics

Significant pairwise differences in tumor incidence between treated groups and controls were determined using Fisher's Exact test followed by adjusted post-hoc testing.

Results

Carcinogenesis study

In the carcinogenesis bioassay (Table 1), several groups of mice were treated with various doses of DB[*a,l*]P (3, 6,12, and 24 nmol/mouse) 3 times per week for 38 weeks. These treatments led to no apparent toxicity as judged by body weight gain (data not shown) and physical observation. The tumor incidences in the ovarian tissues are shown in Figure 1. The ovarian tumors observed are mainly granulosa cell type including both benign (GCT) and malignant tumors (MGCT) (Table 1). At the dose of 3 nmol, the incidence of ovarian tumors was only 25%. Although at the dose of 6 nmol we observed the highest total ovarian tumor incidence (79%), the incidence of malignancy was only 16%. However, at a dose of 12 nmol DB[*a,l*]P induced 75% of the total tumor incidence, and the incidence of MGCT was 65%. The dose of 24 nmol DB[*a,l*]P treatment resulted in the formation of ovarian tumors in 53% of the mice including 47% of MGCT and 6% of GCT; it also resulted in neoplasia in mammary (53%), oral (31%), skin (29%) and lung (12%) tissues of mice.

DB[*a,l*]PDE-DNA adducts formation

In an attempt to demonstrate that the observed ovarian tumors could be resulted from DB[*a,l*]P-induced DNA damage, we detected both (−)-*anti*-cis-DB[*a,l*]PDE-dA and (−)-*anti-trans*-DB[*a,l*]PDE-dA in ovaries of mice orally treated with DB[*a,l*]P using a recently developed LC-MS/MS method (Figure 2).[29] In this bioassay, mice were administered orally (24 nmol) 3 times a week for 5 weeks; DNA were isolated from pooled ovaries (n = 6), which were removed from mice 2, 8, 14, and 28 days after the last administration. We clearly demonstrated that treatment of mice with DB[*a,l*]P resulted in the formation of (−)-*anti-cis*-DB[*a,l*]PDE-dA and (−)-*anti-trans*-DB[*a,l*]PDE-dA adducts in mouse ovary with the *trans* form predominant (Figure 3). The level of adducts were found to decrease dramatically over a week (from 1.6 to 0.84 fmol/10^6 dA for the *trans* adduct, and from 0.8 to 0.15 fmol/10^6 dA for the *cis* adduct), but still detectable 4 weeks (0.72 for the *trans* adduct, and 0.21 for the *cis* adduct) after the last administration. The level of (−)-*anti-trans*-DB[*a,l*]PDE-dA was higher than (−)-*anti-cis*-DB[*a,l*]PDE-dA throughout the entire course of this study.

Discussions

In this study we clearly showed the remarkable carcinogenicity of fjord region DB[*a,l*]P in mouse ovary in a dose-response manner. Based on our results we showed that at doses of 6 and 12 nmol, DB[*a,l*]P predominately induced granulosa cell ovarian tumors in the mouse. At a dose of 24 nmol, DB[*a,l*]P induced ovarian tumors (53%), as well as tumors in mammary gland (53%), oral cavity (31%), skin (29)%, and lung (12%). Our results are consistent with Buters et al, who had reported that following a single dose administered intragastrically to mice, DB[*a,l*]P induced mainly ovarian tumors (71%) and tumors of other sites (less than 47%).[28] Our finding together with previous reports demonstrating the detection of B[*a*]P-DNA adducts and cotinine in ovarian granulose-lutein cells from women exposed to cigarette smoke support the potential role of environmental carcinogens in the development of ovarian cancer.[14,21,31]

DNA-adducts were detected by LC-MS/MS in this study. Mass-spectrometry is able to identify adducts based on their molecular weight and fragmentation patterns; therefore, it is considered the “gold standard” for DNA-adduct identification.[32] The detection of (−)-*anti-cis*-DB[*a,l*]PDE- dA and (−)-*anti-trans*-DB[*a,l*]PDE-dA adducts in ovaries of DB[*a,l*]P-treated mice provides direct evidence that DB[*a,l*]P can be metabolized to its (−)-*anti*-diol epoxide, and this diol epoxide subsequently react with DNA bases to result in DNA

damages in mouse ovary. PAHs that are tumorigenic are considered as procarcinogens because they require metabolic activation to biologically reactive intermediates that can lead to the formation of DNA adducts, which will eventually cause mutation.[33] Although levels of DNA adducts in various organs of rodents treated with various chemical carcinogens do not always correlate with their carcinogenicity;[34] measurement of these adducts provides a method for biomonitoring carcinogen exposure and can provide a risk assessment for susceptibility to carcinogenesis.[33]

Three different pathways have been proposed to be involved in the activation of DB[*a,l*]P; these pathways include: (1) the radical cation pathway (mediated by P450 peroxidases and other peroxidases) to yield depurinating adducts; (2) the diol epoxides pathway (mediated by cytochromes P4501A1/1A2 and 1B1) to yield stable bulky diol epoxide-DNA adducts; and (3) the PAH *ortho*-quinone pathway (mediated by aldo-keto reductases) which results in bulky stable DNA adducts, depurinating adducts, and oxidatively modified DNA lesions. The redox cycling of *ortho*-quinone derivatives of DB[*a,l*]PDE can give rise to reactive oxygen species leading to the formation of the mutagenic lesion, 8-hydroxy-2'-deoxyguanosine (8-oxo-dG).[35] The diol epoxides pathway is the most widely accepted pathway of PAH activation to yield DNA adducts;[33] however, we will aim at examining the possible formation of 8-oxo-dG in the ovary of mice treated with DB[*a,l*]P in the future.

Our results also support the notion that DB[*a,l*]P exerts its biological effects mainly through the diol-epoxides pathway rather than depurinating DNA adducts obtained from radical cation pathway.[36,37] In fact, there is significant evidence that the tumorigenic activity of DB[*a,l*]P is mediated through metabolic acitivation by cytochromes P450 1A1 and 1B1[38] to highly reactive and tumorigenic fjord region diol-epoxides (e.g. DB[*a,l*]PDE)[39] that react strongly with adenine and guanine in cellular DNA (Figure 4),[29,40] especially 1B1-catalyzed formation of DNA-adducts is more critical.[28] In addition, both constituted and inducible forms of 1B1 mRNA was observed in rodents ovary (highest), testis, kidney, heart, brain, thymus, intestine, uterus, and adrenal, but 1A1 mRNA expression in ovary was low before induction.[41,42] Therefore, the capacity of phase I and II enzymes to metabolize DB[*a,l*]P to certain diol epoxides, and level of adduct formation and repair may be involved in its carcinogenic effects in mouse ovary.

The most important electrophilic and reactive DNA-binding diol epoxides specific derived from DB[*a,l*]P are the (+)-*syn*-(11S,12R,13S,14R)- and the (−)-*anti*-(11R,12S,13S,14R)-DB[*a,l*]PDE.[39,43] The carcinogenic activities of these DB[*a,l*]PDEs were linked to the formation of stable DNA adducts[36] that include primarily N_6-dA and to a lesser extent N_2-dG adducts rather than unstable depurinating DNA adducts in native DNA (44). In addition, the metabolic activation of DB[*a,l*]P *in vitro and in vivo* results in the predominant formation of (−)-*anti*-DB[*a,l*]PDE-DNA adducts.[29] Furthermore, the (−)-*anti*-DB[*a,l*]PDE stereoisomer is 3 – 4 times more active than the (+)-*syn*-DB[*a,l*]PDE[45] indicating that the (−)-*anti*-isomer is biologically the most significant diol epoxide derived from DB[a,l]P. Taken together the above mentioned information, we focused initially on the detection of (−)-*anti*-DB[*a,l*]PDE-dA in this study.

The mutagenic activities of the DB[*a,l*]PDE stereoisomers have been extensively studied and reviewed by Luch.[44] Overall, as expected from the higher reactivity of the fjord region diol epoxide with adenine in DNA, dA → dT transversions were dominant in the DB[*a,l*]PDE-treated cells, while in the cells treated with the bay region B[*a*]PDE, dG → dT base substitutions predominated.[46,47] Here, we further postulate that (−)-*anti-trans*-DB[*a,l*]PDE-dA may be more important than (−)-*anti-cis*-DB[*a,l*]PDE-dA because the level of *trans*-adduct is consistently higher than *cis*-adducts throughout 4 weeks after cessation of DB[*a,l*]P treatment.

In soil and sediment samples, the levels of DB[*a,l*]P contents were determined to be in the range of tens to hundreds ppb for samples with different level of pollution, and they are roughly more than 2 orders of magnitude lower than those of B[*a*]P, the gap is reduced by a 40-fold difference in the case of strong contamination.[22] Although DB[*a,l*]P has been detected in cigarette smoke, but has never been quantified. Human exposure to DB[*a,l*]P has been reported.[48] In the case of cigarette smoke, the level of B[*a*]P is ranging from 0.2 to 12.2 μg per 100 cigarettes; therefore, our results suggest that the lifetime exposure of women to PAH, including DB[*a,l*]P via cigarette smoke and environment pollutant, may be at the risk of developing ovarian cancer. In conclusion, our study indicates that ovary is the main target organ in mice treated orally with DB[*a,l*]P; (−)-*anti-tans*-DB[*a,l*]PDE-dA may, in part, account for the carcinogenic activity of DB[*a,l*]P. This animal model can be employed to better understand the mechanisms at the cellular and molecular levels that can account for the induction of ovarian cancer by tobacco carcinogens such as DB[*a,l*]P. Furthermore, it can facilitate the development of novel chemopreventive agents against the development of ovarian cancer.

List of abbreviations

DB[*a,l*]P	dibenzo[*a,l*]pyrene
DB[*a,l*]PDE	dibenzo[*a,l*]pyrene-11,12-dihydrodiol-13,14-epoxide
DMBA	7,12-dimethylbenz[*a*]anthracene
PAH	polycyclic aromatic hydrocarbon
dA	deoxyadenosine
dG	deoxyguanosine
CYP	cytochrome P450 enzymes
MGCT	malignant granulosa cell tumor
GCT	granulosa cell tumor

Acknowledgments

Funding Sources

This study was supported in part by NCI Contract NO2-CB-81013-74, and by seed funds from Penn State Cancer Institute.

References

1. American Cancer Society. Cancer Facts & Figures 2011. Atlanta: American Cancer Society; 2011.
2. Jemal A, Siegel R, Xu J, Ward E. Cancer Statistics 2010. CA: a cancer journal for clinicians. 2010
3. Landen CN Jr, Birrer MJ, Sood AK. Early events in the pathogenesis of epithelial ovarian cancer. J. Clin. Oncol. 2008; 26:995–1005. [PubMed: 18195328]
4. Jabbour HN, Sales KJ, Catalano RD, Norman JE. Inflammatory pathways in female reproductive health and disease. Reproduction. 2009; 138:903–919. [PubMed: 19793840]
5. Coates RJ, Kolor K, Stewart SL, Richardson LC. Diagnostic markers for ovarian cancer screening: not ready for routine clinical use. Clin. Cancer Res. 2008; 14:7575–7576. author reply 7577–7579. [PubMed: 18948387]
6. Viswanath K, Herbst RS, Land SR, Leischow SJ, Shields PG. Tobacco and cancer: an American Association for Cancer Research policy statement. Cancer Res. 2010; 70:3419–3430. [PubMed: 20388799]

7. Zografos GC, Panou M, Panou N. Common risk factors of breast and ovarian cancer: recent view. Int. J. Gynecol. Cancer. 2004; 14:721–740. [PubMed: 15361179]
8. Modugno F, Ness RB, Cottreau CM. Cigarette smoking and the risk of mucinous and nonmucinous epithelial ovarian cancer. Epidemiology. 2002; 13:467–471. [PubMed: 12094103]
9. Terry PD, Miller AB, Jones JG, Rohan TE. Cigarette smoking and the risk of invasive epithelial ovarian cancer in a prospective cohort study. Eur.J. Cancer. 2003; 39:1157–1164. [PubMed: 12736118]
10. Secretan B, Straif K, Baan R, Grosse Y, El Ghissassi F, Bouvard V, Benbrahim-Tallaa L, Guha N, Freeman C, Galichet L, Cogliano V. A review of human carcinogens-- Part E: tobacco, areca, nut, alcohol, coal smoke, and salted fish. lancet Oncol. 2009; 10:1033–1034. [PubMed: 19891056]
11. Karst AM, Drapkin R. Ovarian cancer pathogenesis: a model in evolution. J. Oncol. 2010; 2010:932371. [PubMed: 19746182]
12. Frumovitz M, Schmeler KM, Malpica A, Sood AK, Gershenson DM. Unmasking the complexities of mucinous ovarian carcinoma. Gynecol. Oncol. 2010; 117:491–496. [PubMed: 20332054]
13. Hess V, A'Hern R, Nasiri N, King DM, Blake PR, Barton DP, Shepherd JH, Ind T, Bridges J, Harrington K, Kaye SB, Gore ME. Mucinous epithelial ovarian cancer: a separate entity requiring specific treatment. J. Clin. Oncol. 2004; 22:1040–1044. [PubMed: 15020606]
14. Kurian AW, Balise RR, McGuire V, Whittemore AS. Histologic types of epithelial ovarian cancer: have they different risk factors? Gynecol. Oncol. 2005; 96:520–530. [PubMed: 15661246]
15. Marchbanks PA, Wilson H, Bastos E, Cramer DW, Schildkraut JM, Peterson HB. Cigarette smoking and epithelial ovarian cancer by histologic type. Obstet. Gynecol. 2000; 95:255–260. [PubMed: 10674590]
16. Zhang Y, Coogan PF, Palmer JR, Strom BL, Rosenberg L. Cigarette smoking and increased risk of mucinous epithelial ovarian cancer. Am. J. Epidemiol. 2004; 159:133–139. [PubMed: 14718214]
17. Modugno F, Ness RB, Allen GO. Alcohol consumption and the risk of mucinous and nonmucinous epithelial ovarian cancer. Obstet. Gynecol. 2003; 102:1336–1343. [PubMed: 14662224]
18. Kanter EM, Walker RM, Marion SL, Brewer M, Hoyer PB, Barton JK. Dual modality imaging of a novel rat model of ovarian carcinogenesis. J. Biomed. Opt. 2006; 11:041123. [PubMed: 16965151]
19. Hoyer PB, Davis JR, Bedrnicek JB, Marion SL, Christian PJ, Barton JK, Brewer MA. Ovarian neoplasm development by 7,12-dimethylbenz[a]anthracene (DMBA) in a chemically-induced rat model of ovarian failure. Gynecol. Oncol. 2009; 112:610–615. [PubMed: 19150572]
20. Craig ZR, Davis JR, Marion SL, Barton JK, Hoyer PB. 7,12- dimethylbenz[a]anthracene induces sertoli-leydig-cell tumors in the follicle-depleted ovaries of mice treated with 4-vinylcyclohexene diepoxide. Comparative Med. 2010; 60:10–17.
21. Zenzes MT, Puy LA, Bielecki R. Immunodetection of benzo[a]pyrene adducts in ovarian cells of women exposed to cigarette smoke. Mol. Hum. Reprod. 1998; 4:159–165. [PubMed: 9542974]
22. Kozin IS, Gooijer C, Velthorst NH. Direct Determination of Dibenzo[a,l]pyrene in Crude Extracts of Environmental Samples by Laser-Excited Shpol'skii Spectroscopy. Anal. Chem. 1995; 67:1623–1626.
23. Guttenplan JB, Kosinska W, Zhao ZL, Chen KM, Aliaga C, Deltondo J, Cooper T, Sun YW, Zhang S, Jiang K, Bruggeman R, Sharma AK, Amin S, Ahn K, El-Bayoumy K. Mutagenesis and carcinogenesis induced by dibenzo[a,l]pyrene in the mouse oral cavity: A potential new model for oral cancer. Int. J. Cancer. 2011
24. Mumford ME, Harris DB, Williams K. Indoor air sampling and mutagenicity studies of emissions from unvented coal combustion. Environ. Sci. Technol. 1987; 21:308–311. [PubMed: 22185112]
25. Tong HY, Karasek FW. Quantitation of Polycyclic Aromatic Hydrocarbons in Diesel Exhaust Particulate Matter by High-Performance Liquid Chromatography Fractionation and High-Resolution Gas Chromatography. Anal. Chem. 1984; 56:2129–2134. [PubMed: 6209996]
26. Smith CJ, Hansch C. The Relative Toxicity of Compounds in Mainstream Cigarette Smoke Condensate. Food Chem. Toxicol. 2000; 38:637–646. [PubMed: 10942325]
27. Arif JM, Smith WA, Gupta RC. Tissue distribution of DNA adducts in rats treated by intramammillary injection with dibenzo[a,l]pyrene, 7,12-dimethylbenz[a]anthracene and benzo[a]pyrene. Mutat. Res. 1997; 378:31–39. [PubMed: 9288883]

28. Buters JT, Mahadevan B, Quintanilla-Martinez L, Gonzalez FJ, Greim H, Baird WM, Luch A. Cytochrome P450 1B1 determines susceptibility to dibenzo[a,l]pyrene-induced tumor formation. Chem. Res. Toxicol. 2002; 15:1127–1135. [PubMed: 12230405]
29. Zhang SM, Chen KM, Aliaga C, Sun YW, Lin JM, Sharma AK, Amin S, El-Bayoumy K. Identification and quantification of DNA adducts in the oral tissues of mice treated with the environmental carcinogen dibenzo[a,l]pyrene by HPLC-MS/MS. Chem. Res. Toxicol. 2011; 24:1297–1303. [PubMed: 21736370]
30. Sharma AK, Kumar S, Amin S. A highly abbreviated synthesis of dibenzo[def,p]chrysene and its 12-methoxy derivative, a key Pprecursor for the synthesis of the proximate and ultimate carcinogens of Dibenzo[def,p]chrysene. J. Org. Chem. 2004; 69:3979–3982. [PubMed: 15153038]
31. Zenzes MT, Puy LA, Bielecki R. Immunodetection of cotinine protein in granulosa-lutein cells of women exposed to cigarette smoke. Fertil. Steril. 1997; 68:76–82. [PubMed: 9207588]
32. Poirier MC. Chemical-induced DNA damage and human cancer risk. Nat. Rev. Cancer. 2004; 4:630–637. [PubMed: 15286742]
33. Penning, TM. Polycyclic Aromatic Hydrocarbons: Multiple Metabolic Pathways and the DNA Lesions Formed. Wiley-VCH Verlag GmbH & Co. KGaA; 2010.
34. Helleberg H, Xu H, Ehrenberg L, Hemminki K, Rannug U, Tornqvist M. Studies of dose distribution, premutagenic events and mutation frequencies for benzo[a]pyrene aiming at low dose cancer risk estimation. Mutagenesis. 2001; 16:333–337. [PubMed: 11420402]
35. Park JH, Mangal D, Frey AJ, Harvey RG, Blair IA, Penning TM. Aryl hydrocarbon receptor facilitates DNA strand breaks and 8-oxo-2'-deoxyguanosine formation by the aldo-keto reductase product benzo[a]pyrene-7,8-dione. J. Biol. Chem. 2009; 284:29725–29734. [PubMed: 19726680]
36. Melendez-Colon VJ, Smith CA, Seidel A, Luch A, Platt KL, Baird WM. Formation of stable adducts and absence of depurinating DNA adducts in cells and DNA treated with the potent carcinogen dibenzo[*a*,*l*]pyrene or its diol epoxides. Proc. Natl. Acad. Sci. USA. 1997; 94:13542–13547. [PubMed: 9391062]
37. Xue W, Warshawsky D. Metabolic activation of polycyclic and heterocyclic aromatic hydrocarbons and DNA damage: a review. Toxicol. Appl. Pharmacol. 2005; 206:73–93. [PubMed: 15963346]
38. Luch A, Schober W, Soballa VJ, Raab G, Greim H, Jacob J, Doehmer J, Seidel A. Metabolic activation of dibenzo[a,l]pyrene by human cytochrome P450 1A1 and P450 1B1 expressed in V79 Chinese hamster cells. Chem. Res. Toxicol. 1999; 12:353–364. [PubMed: 10207125]
39. Ralston SL, Lau HH, Seidel A, Luch A, Platt KL, Baird WM. The potent carcinogen dibenzo[a,l]pyrene is metabolically activated to fjord-region 11,12-diol 13,14-epoxides in human mammary carcinoma MCF-7 cell cultures. Cancer Res. 1994; 54:887–890. [PubMed: 8313376]
40. Szeliga J, Dipple A. DNA adduct formation by polycyclic aromatic hydrocarbon dihydrodiol epoxides. Chem. Res. Toxicol. 1998; 11:1–11. [PubMed: 9477220]
41. Shimada T, Sugie A, Shindo M, Nakajima T, Azuma E, Hashimoto M, Inoue K. Tissue-specific induction of cytochromes P450 1A1 and 1B1 by polycyclic aromatic hydrocarbons and polychlorinated biphenyls in engineered C57BL/6J mice of arylhydrocarbon receptor gene. Toxicol. Appl. Pharmacol. 2003; 187:1–10. [PubMed: 12628579]
42. Bhattacharyya KK, Brake PB, Eltom SE, Otto SA, Jefcoate CR. Identification of a rat adrenal cytochrome P450 active in polycyclic hydrocarbon metabolism as rat CYP1B1. Demonstration of a unique tissue-specific pattern of hormonal and aryl hydrocarbon receptor-linked regulation. J. Biol. Chem. 1995; 270:11595–11602. [PubMed: 7744798]
43. Gill HS, Kole PL, Wiley JC, Li KM, Higginbotham S, Rogan EG, Cavalieri EL. Synthesis and tumor-initiating activity in mouse skin of dibenzo[a,l]pyrene syn- and anti-fjord-region diolepoxides. Carcinogenesis. 1994; 15:2455–2460. [PubMed: 7955091]
44. Luch A. On the impact of the molecule structure in chemical carcinogenesis. Exs. 2009; 99:151–179. [PubMed: 19157061]
45. Luch A, Kudla K, Seidel A, Doehmer J, Greim H, Baird WM. The level of DNA modification by (+)-syn-(11S,12R,13S,14R)- and (−)-anti-(11R,12S,13S,14R)-dihydrodiol epoxides of dibenzo[a,l]pyrene determined the effect on the proteins p53 and p21WAF1 in the human mammary carcinoma cell line MCF-7. Carcinogenesis. 1999; 20:859–865. [PubMed: 10334204]

46. Mahadevan B, Dashwood WM, Luch A, Pecaj A, Doehmer J, Seidel A, Pereira C, Baird WM. Mutations induced by (−)-anti-11R,12S-dihydrodiol 13S,14R-epoxide of dibenzo[a,l]pyrene in the coding region of the hypoxanthine phosphoribosyltransferase (Hprt) gene in Chinese hamster V79 cells. Environmental and molecular mutagenesis. 2003; 41:131–139. [PubMed: 12605383]

47. Yoon JH, Besaratinia A, Feng Z, Tang MS, Amin S, Luch A, Pfeifer GP. DNA damage, repair, and mutation induction by (+)-Syn and (−)-anti-dibenzo[a,l]pyrene-11,12- diol-13,14-epoxides in mouse cells. Cancer research. 2004; 64:7321–7328. [PubMed: 15492252]

48. Mumford JL, Li X, Hu F, Lu XB, Chuang JC. Human exposure and dosimetry of polycyclic aromatic hydrocarbons in urine from Xuan Wei, China with high lung cancer mortality associated with exposure to unvented coal smoke. Carcinogenesis. 1995; 16:3031–3036. [PubMed: 8603481]

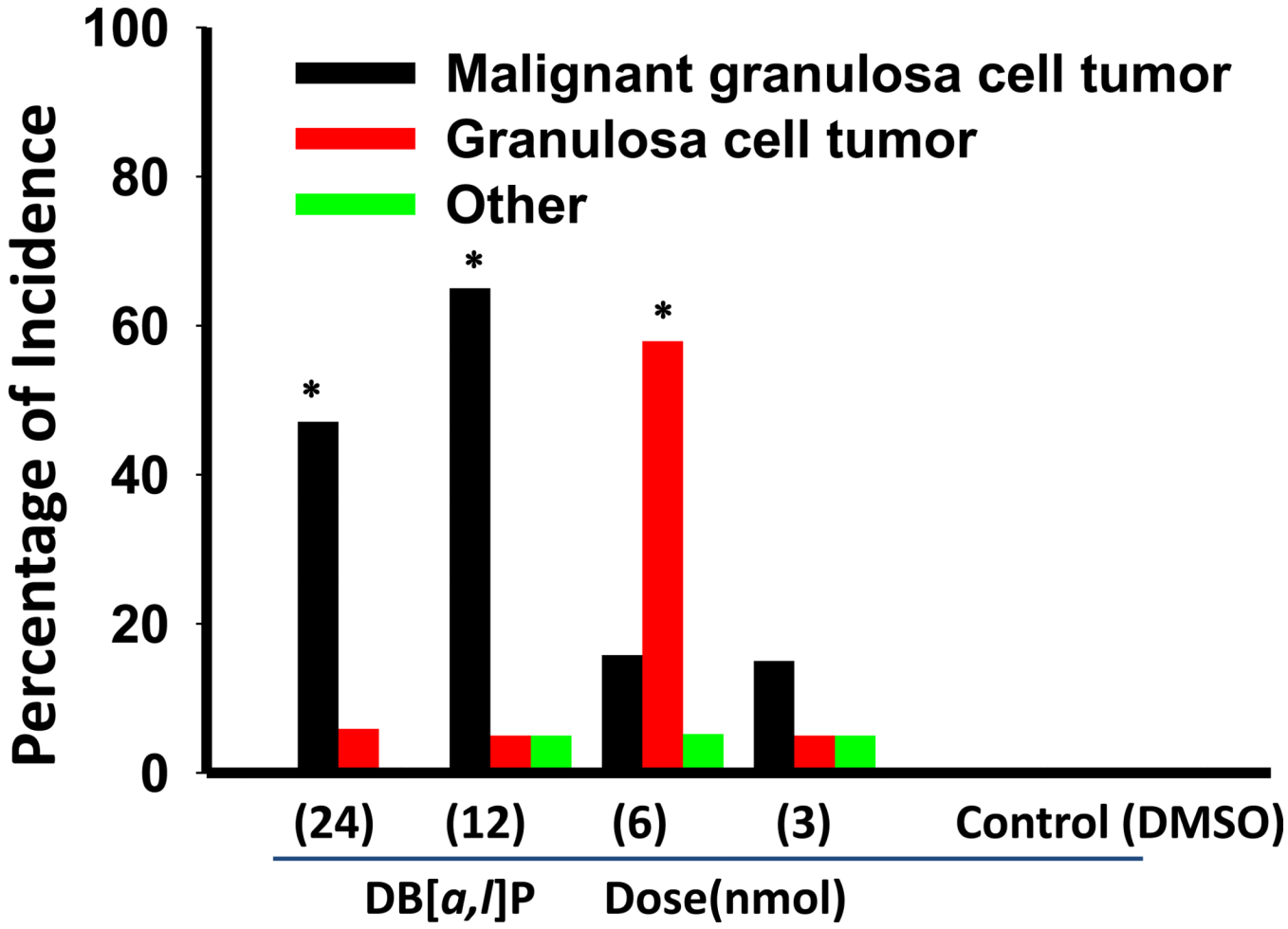

Figure 1.
Incidence of ovarian tumors induced by oral administration of DB[*a*,*l*]P in mouse. *, $p <$ 0.01.

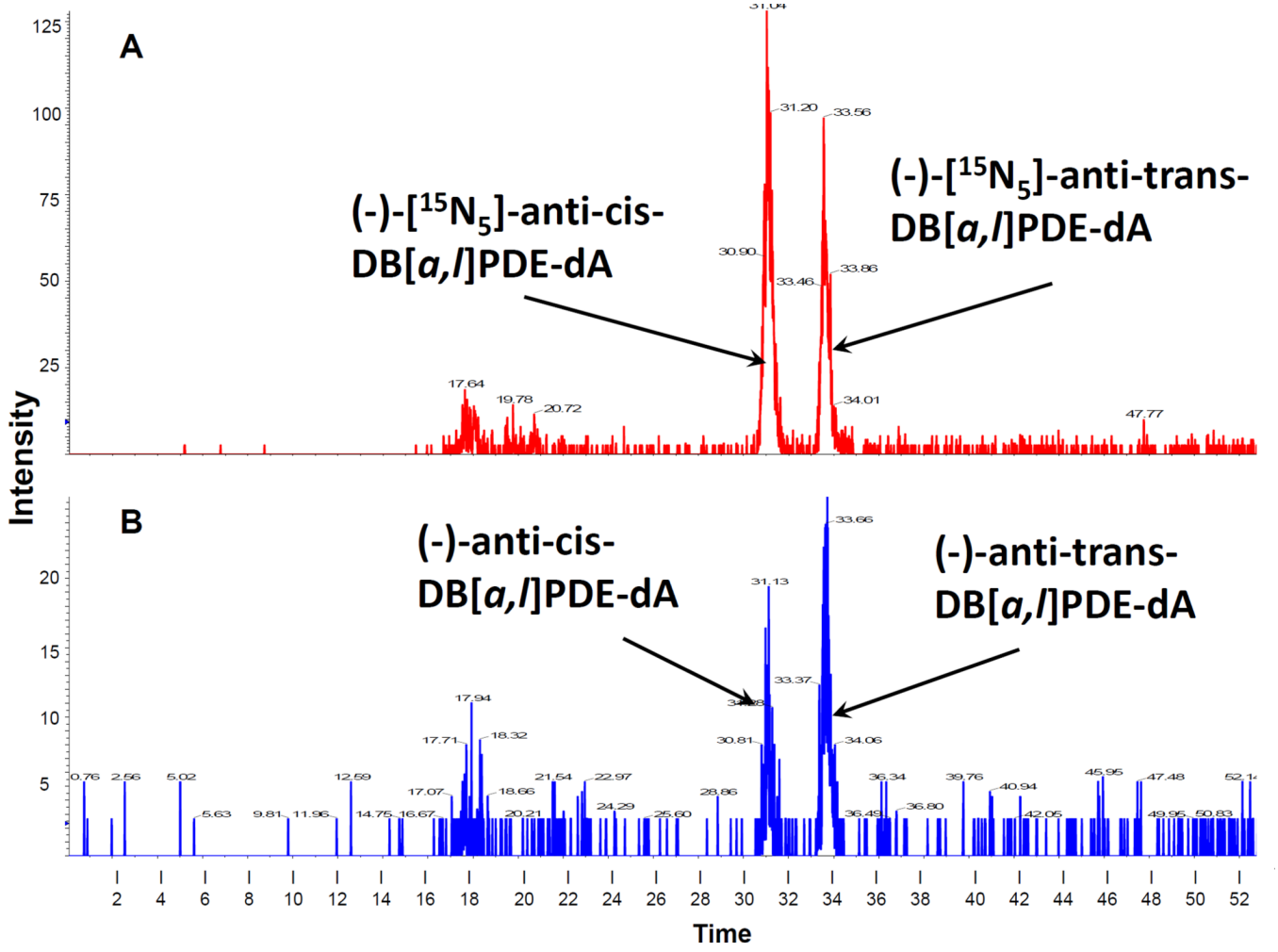

Figure 2.

A representative chromatogram of (−)-*anti*-DB[*a*,*l*]PDE-dA adducts was isolated from the ovary of mice treated with DB[a,l]P and then analyzed by stable isotope dilution HPLC-MS/MS. Chromatogram in red represents the added internal standards (−)-[$^{15}N_5$]-*anti*-DB[*a*,*l*]PDE-dA (**A**), and chromatogram in blue shows hydrolyzed DNA (**B**) obtained from mouse ovary.

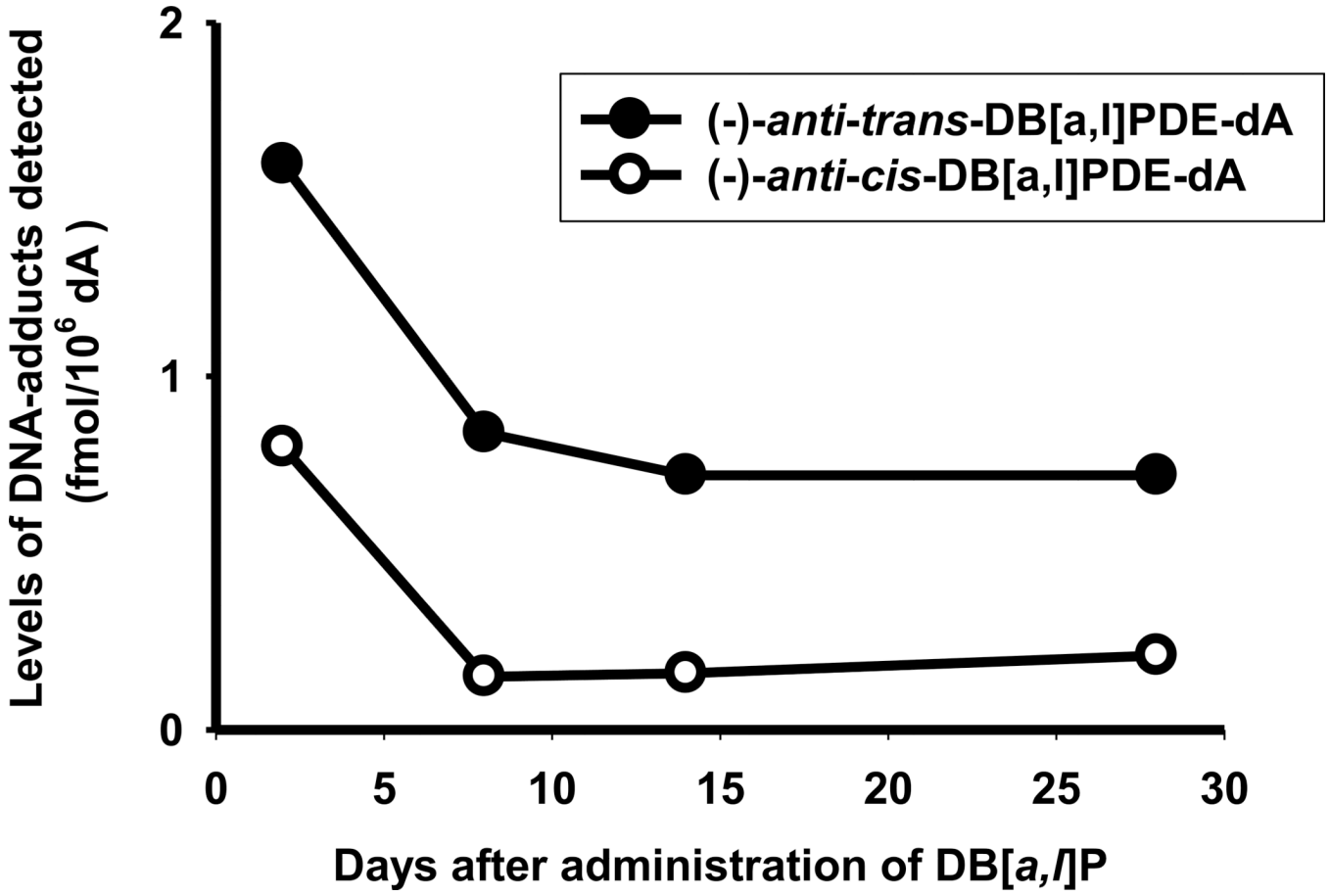

Figure 3.
Levels of (−)-*anti*-DB[*a*,*l*]PDE-dA in ovary of mice at 2 days, and 1, 2, and 4 weeks after cessation of DB[*a*,*l*]P treatment (24 nmol, 3 times/week, for 5 weeks).

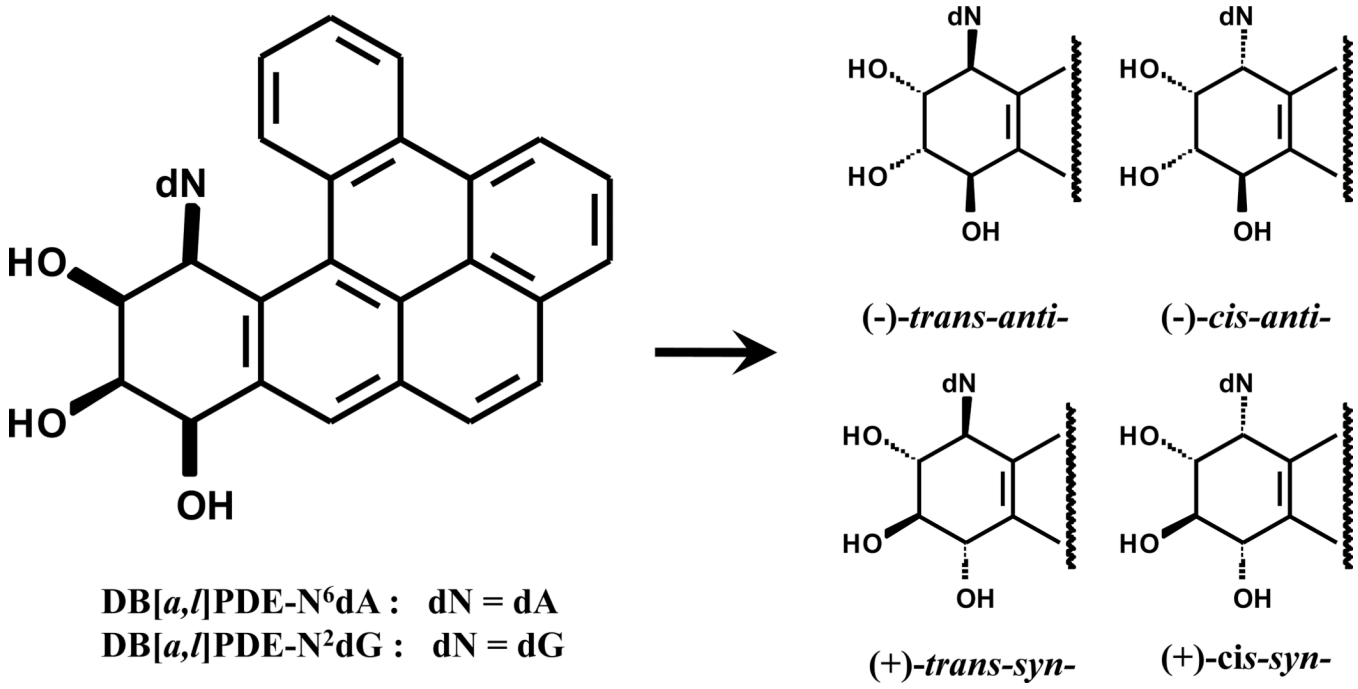

Figure 4.
Structures of DNA adducts derived from DB[*a*,*l*]P found in mammalian cells.

Table 1

Ovarian tumors induced by DB[*a*,*l*]P in female B6C3F1 mice.

DB[a,l]P Treatment	Number of mice	Effective no. of mice[a]	Ovarian Tumors		
			MGCT	GCT	Others
24 nmol	20	17	8 (47)[b,c]	1 (6)	0 (0)
12 nmol	20	20	13 (65)[c]	1 (5)	1 (5)
6 nmol	20	19	3 (16)	11 (58)[c]	1 (5)
3 nmol	20	20	3 (15)	1 (5)	1 (5)
0 nmol	20	19	0 (0)	0 (0)	0 (0)
DMSO	20	20	0 (0)	0 (0)	0 (0)

[a] Mice which died before the first tumor appeared in the study or didn't reach histology due to cannibalism were not counted.

[b] Number in parentheses, percentage.

[c] Significantly induced more than DMSO, $p < 0.01$.